Stability of the plane shear flow of dilute polymeric solutions

Paresh Chokshi and V. Kumaran
Department of Chemical Engineering, Indian Institute of Science, Bangalore 560 012, India

(Received 15 January 2008; accepted 5 December 2008; published online 28 January 2009)

Three variants of Oldroyd-B model are analyzed for stability of the base profile in plane Couette flow of dilute polymeric fluid at moderate Reynolds number. The stability to two-dimensional disturbances is analyzed for the linearized problem as well as the weakly nonlinear flow. We begin with the classical Oldroyd-B model with emphasis on the disturbances with axial wavenumber $\alpha \sim \mathrm{Re}^{1/2}$, where Re is the Reynolds number based on maximum velocity and channel width. For linearly stable flow, the finite amplitude stability is analyzed using the equilibrium flow method, wherein the nonlinear flow is assumed to be at the transition point. For the classical Oldroyd-B fluid, the threshold kinetic energy for the equilibrium wall mode disturbances is found to be higher for the viscoelastic fluid than for the Newtonian fluid. In the second variant, the Oldroyd-B model with additional artificial diffusivity is studied. In this model, the diffusion modes, not present in the classical Oldroyd-B model, are introduced. For large wavenumber disturbances, the diffusion modes become the slowest decaying modes in comparison to the wall modes. The threshold energy for the diffusive Oldroyd-B model is smaller than that for the Newtonian fluid. The third variant of the Oldroyd-B model accounts for the nonhomogeneous polymer concentration coupled with the polymeric stress field. While the base profile is linearly stable for the first two models, the nonhomogeneous Oldroyd-B fluid exhibits an instability in the linear analysis. The "concentration mode" becomes unstable when the fluid Weissenberg number exceeds a certain transition value. This mode of instability, driven by the stress-induced fluctuations in polymer number density, renders the uniform polymer concentration profile unstable leading to the well-known phenomenon of flow-induced demixing. © *2009 American Institute of Physics*. [DOI: 10.1063/1.3063893]

I. INTRODUCTION

Interactions between the hydrodynamics and the polymer chains have been an object of research for many decades. Several investigations have been carried out in different flow regimes, many motivated by and with the intention to gain an in-depth understanding of the familiar phenomenon of turbulent drag reduction by polymer molecules in a fully developed turbulent flow. In turbulent flows, the flow in the region nearby the wall is laminar. Hence, the influence of polymer chains on laminar flow is believed to help elucidate the role of polymers in wall-bounded turbulent flows. The analysis of stability is the classical approach to study the transition to turbulence, although the gap between the instability and the fully developed turbulence is one of the major challenges in fluid mechanics.

First, we briefly review the role of stability analysis in addressing the problem of laminar to turbulent transition in a plane Couette flow of a Newtonian fluid. The transition in this apparently simple shear flow is rather complex and is not yet understood completely. The difficulty is due to the fact that the plane Couette flow is linearly stable, whereas in practice the flow undergoes transition at a finite Reynolds number. At high Reynolds number, the viscous effects in disturbance flow field are confined to a thin layer of thickness $O(\alpha\,\mathrm{Re})^{-1/3}$ times the channel width.[1,2] This layer is known as the wall layer and the disturbance modes the wall modes. Here, α is the axial wavenumber of perturbation and Re is the Reynolds number. Based on the stability analysis of the wall modes, it is now widely accepted that the plane Couette flow is linearly stable and the observed transition to turbulence is triggered by the disturbances of finite amplitude.[3] Due to the lack of transition Reynolds number, the finite amplitude state bifurcates from infinity resulting in a subcritical instability leading to transition to turbulence. The earlier weakly nonlinear analyses suggested the presence of two-dimensional (2D) finite amplitude instability characterized by a threshold amplitude.[4,5] However, numerical simulations that examine the time evolution of the 2D disturbances in a plane Couette flow do not show the existence of the finite amplitude instability. The simulations suggest that the three-dimensional (3D) effect is necessary for the initial disturbance to develop and instability and result in a sustained turbulence.[6] These numerical solutions do not confirm the existence of 2D finite amplitude instability predicted by the weakly nonlinear stability analyses of Refs. 4 and 5. This led to search for 3D nonlinear solutions for a plane Couette flow using homotopy from the other flows such as plane Poiseuille and Taylor–Couette flows. Both steady and traveling-wave solutions have been discovered[7,8] that match with the experimental data on transition to turbulence. Additionally, the existence of 2D steady solution as the equilibrium state has also been shown, although its participation in transition to turbulence remains doubtful.[9] By and large it is now established that in the absence of a linear instability, sustained turbulence is generated from a 3D finite amplitude

state. In the present study, we analyze the linear and weakly nonlinear stability of a viscoelastic flow. Since it is known that a viscoelastic flow does exhibit linear instability, we restrict our analysis to 2D disturbances. For a Newtonian flow, the finite amplitude 2D traveling-wave solution exists as the equilibrium state.[4,5] For this case, the threshold energy for the subcritical transition was shown to be minimum for critical disturbances with wavenumber $\alpha \sim \mathrm{Re}^{1/2}$. In the present analysis, we seek to examine the influence of polymer chains on the threshold energy.

Motivated by the phenomenon of polymer melt fracture during extrusion, the stability of inertialess flow of various model polymers has been analyzed by many in order to establish the flow instability as the cause for observed breakage. For a plane Couette flow in the limit of zero Reynolds number, Gorodtsov and Leonov[10] showed analytically that a viscoelastic fluid described using the upper convected Maxwell (UCM) model is stable to infinitesimal disturbances for any arbitrary Weissenberg number (the relaxation time of dumbbells nondimensionalized with the flow time scale). Renardy[11] provided a rigorous proof of linear stability of this flow. Also, for small nonzero Reynolds number, the flow is found to be linearly stable.[12,13] However, the nonlinear interactions of the polymer stress and the fluid velocity field can give rise to finite amplitude instability. For linearly stable flows, the methodology proposed by Reynolds and Potter[14] can be used to find the finite amplitude equilibrium solution of the disturbance equations. Using this method of equilibrium flow for polymer melts described as UCM fluids, Morozov and Saarloos[15] estimated the threshold amplitude for subcritical transition in small Reynolds number flow. The convergence of the threshold amplitude was shown by incorporation of higher order terms in the amplitude equation. For dilute solutions, the presence of small amount of polymer molecules in otherwise Newtonian fluid has profound effect on the flow behavior. The addition of long-chain molecules significantly modifies the stability characteristics of a plane Poiseuille flow.[16,17] The effect of fluid elasticity on the critical Reynolds number for this flow shows an opposite behavior around a critical elasticity parameter, below which the effect is destabilizing and above which it is stabilizing.

As we continue the Newtonian wall modes to viscoelastic fluid, we observe that for axial wavenumber of the order $(\mathrm{Re}^{1/2})$, the discrete wall modes are interfered by the presence of the continuous spectra. The disturbance equation for the Oldroyd-B fluid exhibits singularity along the two continuous spectra of eigenmodes which are always stable.[13,18] The singular eigenfunctions corresponding to these continuous spectra are expressed in terms of Dirac distribution functions for polymer stress components.[19] Being divergence-free, these solutions do not impact the fluid flow field. While the singular modes are linearly stable, there is an indication of transient growth due to the non-normal nature of operator in the Oldroyd-B model. Kupferman[19] discussed the need to introduce a weak artificial diffusivity to attenuate strong oscillations in polymer stress field in cross-flow direction. A rigorous proof of stress diffusion being necessary for the existence of solutions for viscoelastic fluids is given in Ref. 20. For time-dependent numerical simulations of viscoelastic flows, an additional artificial diffusion of polymer conformation tensor is usually incorporated in the classical Oldroyd-B model to regularize the governing equations.[21,22] Incorporating diffusion with any arbitrary small amount of diffusivity D is found to destroy the continuous spectra.[17,18]

Most polymeric flows in reality are nonhomogeneous; i.e., the velocity gradient, the polymer distribution, and the components of conformation tensor and hence the stress vary spatially in the flow domain. Different parts of a long-chain molecule can be subjected to different forces and polymer number density can be different near the wall and away from the wall. In the diffusive Oldroyd-B model, while the diffusion of polymer conformation tensor is allowed, the polymer concentration is assumed to be spatially uniform. Physically, diffusion is a consequence of local inhomogeneity in concentration. It is, therefore, appropriate to incorporate the polymer concentration fluctuations in the stability analysis. Moreover, the homogeneous model, with uniform polymer distribution, fails to capture the observed phenomenon of polymer migration induced by the stress gradient. Hence, a model considering the nonuniform polymer number density n as an additional variable should be more realistic. A model capturing the rheology and mass transfer phenomena in dilute polymer solutions with spatially varying distribution of elastic dumbbell molecules has been derived by a number of researchers using the principals of kinetic theory[23] as well as using the principles of continuum mechanics[24] and nonequilibrium thermodynamics.[25] The comparison and the compatibility of the outcome of the different approaches to derive a continuum scale model for nonhomogeneous polymer solution are discussed comprehensively by Beris and Mavrantzas.[26] The nonhomogeneous Oldroyd-B model exhibits stress-concentration coupling and hence accounts for stress-induced migration of polymer molecules apart from polymer chain diffusion. The stability of the flow of nonhomogeneous polymer solutions is not widely studied. Apostolakis *et al.*[27] analyzed the stress-induced migration of the polymer molecules in the base flow in Taylor–Couette geometry. The migration, which is away from the outer cylinder toward the inner one, is in agreement with the experimental observations.[28,29] The role of concentration fluctuations in Taylor–Couette flow instability was found to be dramatic. Unstable modes qualitatively different from that present in the flow of uniform polymer solution were found to destabilize the system at lower elasticity parameter (Deborah number, the dimensionless fluid relaxation time) than its critical value for the homogeneous Oldroyd-B fluid.[27] Other works that make use of the coupled distribution between the polymer concentration and stress include Refs. 30–32. The inertialess flow of Maxwell fluid is stable for all values of elasticity parameter.[10] For the nonhomogeneous polymer concentration and a wall slip, Black and Graham[31] found an unstable "concentration mode" leading to an instability at a finite Weissenberg number.

In the present work, we perform linear and weakly nonlinear stability analyses of the planar shear flow of dilute polymeric solutions. The viscoelasticity is described by three progressively rigorous variants of an Oldroyd-B model, viz., the classical Oldroyd-B fluid, uniform Oldroyd-B fluid with

stress diffusivity, and nonhomogeneous Oldroyd-B fluid. The later model allows for the concentration fluctuations coupled with the polymeric stress. In the larger context, this coupling is at the center of many mechanisms to explain various stress-induced phenomena in the field of polymer physics. Flow can greatly influence the phase behavior of polymeric solutions and blends. Shear-induced mixing and demixing both have been observed depending on the temperature.[33,34] Various effects of demixing such as polymer chain migration in curvilinear flows, stress-induced diffusion in wall-bounded flows, and concentration fluctuations leading to turbidity have all been investigated thoroughly over last few decades. The comprehensive reviews of flow-induced transformations in the structure of polymeric fluids have been presented by Rangle-Nafaile *et al.*[35] and Larson.[36] A more recent review can be found in Ref. 37. As we will see later in this paper, the uniform concentration profile tends to become unstable beyond a certain Weissenberg number leading to demixing manifested by an enhanced scattering. This work finds its significance in the context of shear-induced transformations in polymeric fluids reported by Larson.[36] Beginning with the quasithermodynamic description introduced by Rangle-Nafaile *et al.*,[35] the theoretical framework for the flow-induced concentration fluctuations has undergone many refinements. Much of the present understanding is based on the statistical mechanical theory of Helfand and Fredrickson[38] and its extensions to the continuum scale two-fluid models by many investigators (Onuki,[39,40] Doi and Onuki,[41] Milner,[42] Bhave *et al.*,[23] Mavrantzas and Beris,[25] etc.). Recently, Minale[43] employed the modified two-fluid model to predict a true phase separation induced by a steady flow in polymer solutions. The coexistence of shear-induced phases and their instability in surfactant systems has been studied by Olmsted and Lu[44] and Fielding and Olmsted.[45] Overall, the present literature is rich in studies in flow-induced phase transitions and structural changes in polymeric and other complex fluids. This paper makes a contribution toward the onset of instability in uniform concentration profile leading to demixing and possibly phase separation.

The rest of this paper is organized as follows. The governing equations of variants of the Oldroyd-B model used in the present study are provided in Sec. II. The methodology and the solution procedure are explained in Sec. III. In Sec. IV, the results of the linear and weakly nonlinear stability analyses are discussed for the classical Oldroyd-B, the diffusive Oldroyd-B, and the nonhomogeneous Oldroyd-B fluids. Section V summarizes important conclusions from the present work.

II. MODEL EQUATIONS

A. Classical Oldroyd-B model

The system consists of a plane Couette flow of an incompressible viscoelastic fluid with zero shear viscosity η occupying the domain $0<y^*<L$ in the cross-stream direction, with top plate moving with constant axial velocity $\bar{v}_x^*=V$ and bottom plate held stationary. The fluid continuity equation and momentum balance equation, upon nondimensionalizing velocity with V, distance with L, time with L/V, pressure with ρV^2, and stresses with $\eta V/L$, become

$$\nabla \cdot \mathbf{v} = 0, \tag{1}$$

$$\partial_t \mathbf{v} + \mathbf{v} \cdot \nabla \mathbf{v} = -\nabla p + \frac{1}{\mathrm{Re}} \nabla \cdot \boldsymbol{\tau}^s + \frac{1}{\mathrm{Re}} \nabla \cdot \boldsymbol{\tau}^p. \tag{2}$$

The Reynolds number is defined, based on solution viscosity, as $\mathrm{Re}=\rho VL/\eta$. For viscoelastic fluid, the stress tensor consists of viscous stress ($\boldsymbol{\tau}^s$) and polymeric stress ($\boldsymbol{\tau}^p$). The viscous stress arising due to the solvent viscosity (η_s) is given by Newton's law,

$$\boldsymbol{\tau}^s = \beta [\nabla \mathbf{v} + (\nabla \mathbf{v})^T], \tag{3}$$

where the superscript T indicates the transpose and $\beta = \eta_s/\eta$ indicates the solvent contribution to the solution viscosity η, where $\eta=\eta_s+\eta_p$. The polymer contribution is indicated by $(1-\beta)$, which is proportional to the polymer concentration in the solution.

The classical Oldroyd-B model can be derived from the microscopic description using the concepts of kinetic theory[46] as well as from the phenomenology, such as Maxwell's spring-dashpot model, with the assumption of spatially uniform configuration distribution of the polymer molecules in homogeneous flow field. The polymer chain is microscopically described as a linear elastic dumbbell with two beads at ends connected via an entropic spring. The polymer constitutive relation is expressed in terms of statistically averaged properties of chain over all possible configurations in the flow field. The characteristic length scale of a polymer chain is end-to-end distance $\langle \mathbf{Q}\cdot\mathbf{Q}\rangle^{1/2}$. The conformation tensor, defined as $c_{ij}^*=\langle Q_i Q_j\rangle$, is obviously a symmetric and positive definite tensor. Here, the superscript "$*$" indicates a dimensional quantity. The conformation tensor is governed by a simple relaxation law with time constant λ toward thermal equilibrium conformation $\mathbf{c}^{*\mathrm{eq}}$,

$$\mathcal{D}_t \mathbf{c}^* = -\frac{(\mathbf{c}^* - \mathbf{c}^{*\mathrm{eq}})}{\lambda}. \tag{4}$$

In order to make the above constitutive relation reference-frame indifferent, the material time derivative is the upper convected derivative defined as

$$\mathcal{D}_{t^*} \mathbf{c}^* = \partial_{t^*} \mathbf{c}^* + \mathbf{v}^* \cdot \nabla \mathbf{c}^* - \mathbf{c}^* \cdot (\nabla \mathbf{v}^*) - (\nabla \mathbf{v}^*)^T \cdot \mathbf{c}^*. \tag{5}$$

Here, the equilibrium conformation $\mathbf{c}^{*\mathrm{eq}}=(k_B T/H)\delta_{ij}$ and the relaxation time of the viscoelastic fluid $\lambda=\xi/H$, with H being the spring constant of the elastic dumbbells, ξ being microscopic friction coefficient of beads, and $k_B T$ being the thermal energy.

The polymeric stress is proportional to the departure of chain conformation from thermal equilibrium conformation,

$$\tau^{*p} = \frac{\eta_p H}{\lambda k_B T}(\mathbf{c}^* - \mathbf{c}^{*\mathrm{eq}}). \tag{6}$$

Upon nondimensionalizing $\mathbf{c}$ with $(k_B T/H)$, $\boldsymbol{\tau}^p$ with $\eta V/L$ and time with L/V, the classical Oldroyd-B model is described by

$$\mathcal{D}_t \mathbf{c} = -\frac{(\mathbf{c}-\mathbf{I})}{W}, \tag{7}$$

$$\boldsymbol{\tau}^p = (1-\beta)\frac{(\mathbf{c}-\mathbf{I})}{W}, \tag{8}$$

where the Weissenberg number, which is indicative of the fluid elasticity, is defined as $W=\lambda V/L$ and $\mathbf{I}$ is an identity tensor. The overall fluid governing equations thus become

$$\partial_t \mathbf{v} + \mathbf{v}\cdot\nabla\mathbf{v} = -\nabla p + \frac{\beta}{\mathrm{Re}}\nabla^2\mathbf{v} + \frac{(1-\beta)}{\mathrm{Re}\,W}\nabla\cdot\mathbf{c}, \tag{9}$$

$$\partial_t \mathbf{c} + \mathbf{v}\cdot\nabla\mathbf{c} - \mathbf{c}\cdot(\nabla\mathbf{v}) - (\nabla\mathbf{v})^T\cdot\mathbf{c} = -\frac{(\mathbf{c}-\mathbf{I})}{W}. \tag{10}$$

B. Diffusive Oldroyd-B model

The hyperbolic nature of the evolution equation for the conformation tensor [Eq. (7)] results in the perturbation equation with singularities leading to branch cut in the eigenvalue space.[13] Moreover, the above classical Oldroyd-B model poses numerical problems while performing time-dependent simulation of the Oldroyd-B fluid. Hence, it is generally agreed to introduce an artificial diffusivity to stabilize the numerical scheme. Thus, the classical Oldroyd-B model is modified by an additional diffusive term in the governing equation for the conformation tensor as

$$\mathcal{D}_t \mathbf{c} = -\frac{(\mathbf{c}-\mathbf{I})}{W} + \frac{1}{\mathrm{Pe}}\nabla^2\mathbf{c}, \tag{11}$$

where the Péclet number is defined as $\mathrm{Pe}=LV/D_{\mathrm{tr}}$, with D_{tr} being the translational diffusivity of the polymer chain.

The addition of diffusive term necessitates boundary conditions for the conformation tensor to be specified. The state of polymer chain and the extent of its stretching at the walls remain uncertain. The Monte Carlo simulations of equilibrium and nonequilibrium distributions of polymer solutions confined between the parallel plates indicate that the presence of a solid wall affects configurations of the polymer molecules in a narrow region of thickness comparable to the average radius of gyration of polymer molecules close to the wall.[47] Different researchers have used different types of boundary conditions for the components of the conformation tensor. Sureshkumar and Beris[16] applied the classical Oldroyd-B governing equation (7) at the walls. Black and Graham[31] employed no-flux boundary condition, i.e., conformational flux $\mathbf{J}_c=\mathbf{vc}-(1/\mathrm{Pe})\nabla\mathbf{c}=0$ across the walls. Bhave *et al.*[23] introduced the molecular orientation near wall simply by requiring the elastic dumbbells to be parallel to the wall as a boundary condition. Thus, the polymer chain is assumed to be stretched along the flow direction with its length Q_0 as an arbitrary parameter. In the present study, we use the first two kinds of boundary conditions, i.e., enforce the Oldroyd-B governing equation without diffusion term at the walls, and specify zero flux of polymer conformation in the wall-normal direction.

C. Nonhomogeneous polymer solution model

Since the polymer chain diffusion is a consequence of local nonhomogeneity, previous models, which are based on the assumption of spatial uniformity of polymer distribution, are not reasonable when the diffusion effects are taken into consideration. A model capturing the rheology and mass transfer phenomena in dilute polymer solution with spatially varying distribution has been derived by some researchers using the kinetic theory approach[23] as well as using the principles of continuum mechanics[24] and the nonequilibrium thermodynamics.[25] This model exhibits stress-concentration coupling and hence accounts for stress-induced migration of polymer molecules apart from molecular diffusion. The nondimensional momentum balance equation and the polymer constitutive relation are as follows:

$$\partial_t \mathbf{v} + \mathbf{v}\cdot\nabla\mathbf{v} = -\nabla p + \frac{\beta}{\mathrm{Re}}\nabla^2\mathbf{v} + \frac{1}{\mathrm{Re}}\nabla\cdot\boldsymbol{\tau}^p, \tag{12}$$

$$\boldsymbol{\tau}^p = (1-\beta)\frac{(\mathbf{C}-n\mathbf{I})}{W}, \tag{13}$$

where n is polymer number density. Here, we use the number density weighted conformation tensor $\mathbf{C}$ $(=n\mathbf{c})$, as against the single chain conformation tensor $\mathbf{c}$. The governing equation for $\mathbf{C}$ is

$$\mathcal{D}_t \mathbf{C} = -\frac{(\mathbf{C}-n\mathbf{I})}{W} + \frac{1}{\mathrm{Pe}}\nabla^2\mathbf{C}. \tag{14}$$

An alternate expression in terms of polymeric stress is

$$\boldsymbol{\tau}^p + W\mathcal{D}_t\boldsymbol{\tau}^p + (1-\beta)\left[\frac{Dn}{Dt} - \frac{1}{\mathrm{Pe}}\nabla^2 n\right]\mathbf{I} = \frac{W}{\mathrm{Pe}}\nabla^2\boldsymbol{\tau}^p + (1-\beta)n\dot{\gamma}, \tag{15}$$

where $\dot{\gamma}$ is the rate-of-strain tensor, $\dot{\gamma}=[\nabla\mathbf{v}+(\nabla\mathbf{v})^T]$. Finally, the mass conservation equation for the polymer number density is as follows:

$$\frac{Dn}{Dt} = \frac{1}{\mathrm{Pe}}\nabla^2 n - \frac{1}{(1-\beta)}\frac{W}{\mathrm{Pe}}\nabla\nabla:\boldsymbol{\tau}^p. \tag{16}$$

An alternate form in terms of $\mathbf{C}$ is

$$\frac{Dn}{Dt} = \frac{2}{\mathrm{Pe}}\nabla^2 n - \frac{1}{\mathrm{Pe}}\nabla\nabla:\mathbf{C}. \tag{17}$$

The polymer mass flux is given as

$$\mathbf{J} = -\left[\frac{1}{\mathrm{Pe}}\nabla n - \frac{1}{(1-\beta)}\frac{W}{\mathrm{Pe}}\nabla\cdot\boldsymbol{\tau}^p\right] \tag{18}$$

$$= -\left(\frac{2}{\mathrm{Pe}}\nabla n - \frac{1}{\mathrm{Pe}}\nabla\cdot\mathbf{C}\right). \tag{19}$$

The boundary conditions for the conformation tensor have been discussed in Sec. II B. The first kind of boundary condition requires the conformation equation (14) with $\mathrm{Pe}\to\infty$ to be satisfied at the walls. The second kind specifies zero conformation flux, $d_y\mathbf{C}=0$, at the surfaces. The polymer concentration satisfies the typical no-flux boundary condition

at the surfaces, i.e., $\mathbf{J}=-2\nabla n+\nabla\cdot\mathbf{C}=0$, in the wall-normal direction.

III. STABILITY ANALYSIS

For all three models discussed above, the steady-state solution for the plane Couette flow is same and is as follows:

$$\bar{\mathbf{v}}=(y,0,0), \tag{20}$$

$$\bar{\mathbf{c}}=\begin{pmatrix}1+2W^2 & W & 0\\ W & 1 & 0\\ 0 & 0 & 1\end{pmatrix},\quad \bar{\boldsymbol{\tau}}^p=(1-\beta)\begin{pmatrix}2W & 1 & 0\\ 1 & 0 & 0\\ 0 & 0 & 0\end{pmatrix}. \tag{21}$$

This base flow satisfies both the no-flux for conformation tensor as well as the classical Oldroyd-B equation at the walls. For the case of nonhomogeneous solutions, the base-state polymer concentration is uniform with $\bar{n}=n_0=1$. For this model, the mass-averaged conformation tensor is $\bar{\mathbf{C}}=n_0\bar{\mathbf{c}}$. We like to note that the base profile for polymer concentration will be nonuniform if one chooses to use the boundary conditions suggested by Bhave *et al.*,[23] i.e., $\bar{C}_{xx}=n_wQ_0^2$, $\bar{C}_{xy}=\bar{C}_{xx}=0$ at the walls.

A. Linear stability

To study the temporal stability, the steady-state profile is superimposed with the 2D classical normal mode perturbations of infinitesimally small amplitude of the form

$$\phi'(x,y,t)=\tilde{\phi}(y)e^{i\alpha(x-ct)}, \tag{22}$$

where the general variable $\phi=[\mathbf{v},\mathbf{c},n]^T$, α is the real-valued axial wavenumber, and c is the complex wavespeed, the sign of whose imaginary part is indicative of growth or decay of the infinitesimal disturbance. Upon linearizing, we get the following governing equations for disturbance eigenfunctions in the classical Oldroyd-B model:

$$i\alpha(y-c)\tilde{v}_x+\tilde{v}_y y=-i\alpha\tilde{p}+\frac{\beta}{\mathrm{Re}}(d_y^2-\alpha^2)\tilde{v}_x+\frac{(1-\beta)}{\mathrm{Re}\ W}(d_y\tilde{c}_{xy}+i\alpha\tilde{c}_{xx}), \tag{23}$$

$$i\alpha(y-c)\tilde{v}_y=-d_y\tilde{p}+\frac{\beta}{\mathrm{Re}}(d_y^2-\alpha^2)\tilde{v}_y+\frac{(1-\beta)}{\mathrm{Re}\ W}(d_y\tilde{c}_{yy}+i\alpha\tilde{c}_{xy}), \tag{24}$$

$$i\alpha(y-c)\tilde{c}_{xx}-2i\alpha(1+2W^2)\tilde{v}_x-2Wd_y\tilde{v}_x-2\tilde{c}_{xy}=-\frac{1}{W}\tilde{c}_{xx}, \tag{25}$$

$$i\alpha(y-c)\tilde{c}_{xy}-i\alpha(1+2W^2)\tilde{v}_y-d_y\tilde{v}_x-\tilde{c}_{yy}=-\frac{1}{W}\tilde{c}_{xy}, \tag{26}$$

$$i\alpha(y-c)\tilde{c}_{yy}-2i\alpha W\tilde{v}_y-2d_y\tilde{v}_y=-\frac{1}{W}\tilde{c}_{yy}. \tag{27}$$

Substituting for the components of the conformation tensor obtained by solving the algebraic equations (25)–(27) in the fluid momentum balance equations and eliminating pressure results in a single fourth order ordinary differential equation,

$$(1-\beta)[(S^2D^2-2i\alpha WSD-2\alpha^2W^2-\alpha^2S^2)(D^2+2i\alpha WD-2\alpha^2W^2-\alpha^2)\tilde{v}_y]+\beta[S^3(D^2-\alpha^2)^2\tilde{v}_y]-i\alpha\,\mathrm{Re}(y-c)S^3(D^2-\alpha^2)\tilde{v}_y=0, \tag{28}$$

where $D=d_y$ and $S=1+i\alpha W(y-c)$. The governing equations are supplemented with no-slip conditions at the walls: $\tilde{v}_y=d_y\tilde{v}_y=0$ at $y=0$ and $y=1$.

For the diffusive Oldroyd-B model, a diffusivity term $(1/\mathrm{Pe})(d_y^2-\alpha^2)\tilde{c}_{ij}$ is added on the right-hand side of Eqs. (25)–(27). The conformation equations for the nonhomogeneous model are similar to that for the diffusive model, with $\tilde{\mathbf{c}}$ being replaced by $\tilde{\mathbf{C}}$ and an additional term $(1/W)\tilde{n}\,\mathbf{I}$ on the right-hand side. We do not write the equations for $\tilde{\mathbf{C}}$ to avoid repetition. The disturbance equation for the polymer number density in terms of $\tilde{\mathbf{C}}$ is given as

$$i\alpha(y-c)\tilde{n}+\tilde{v}_yd_y\bar{n}=\frac{2}{\mathrm{Pe}}(d_y^2-\alpha^2)\tilde{n}-\frac{1}{\mathrm{Pe}}(d_y^2\tilde{C}_{yy}-\alpha^2\tilde{C}_{xx}+2i\alpha d_y\tilde{C}_{xy}). \tag{29}$$

B. Finite amplitude instability

For finite amplitude disturbances, the convective nonlinearities in the governing equations manifest themselves through nonlinear self-interactions of eigenfunctions of the linear analysis. The nonlinear analysis constructs a branch to the stability curve in the amplitude direction using an equation, referred to as the Landau equation, of the form

$$\frac{dA}{dt}=s^{(0)}A+s^{(1)}A|A|^2+\cdots, \tag{30}$$

where $s^{(0)}$ is the linear growth of small disturbances and $s^{(1)}$ is the higher order correction to the linear growth rate, known as the Landau constant. In terms of wavespeed $s^{(0)}=\alpha c_i$, where c_i is the imaginary part of the complex wavespeed. For flows which are linear unstable, $s^{(1)}$ provides the nature of bifurcation at the transition point, that is, $c_i=0$. Following the formulations given by Stuart[48] and Watson,[49] in the vicinity of the transition point the flow variables are expanded in harmonic-amplitude series,

$$\phi(x,y,t)=\bar{\phi}(y)+\sum_{k=0}^{\infty}\sum_{n=k,n\neq 0}^{\infty}[A(t)]^n\times[\tilde{\phi}^{(k,n)}(y)e^{ik(\alpha x+\omega t)}+\tilde{\phi}^{(k,n)^\dagger}(y)e^{-ik(\alpha x+\omega t)}], \tag{31}$$

where $\phi=[\mathbf{v},\mathbf{c},n]$, $\bar{\phi}$ is the base flow quantity, and superscript "†" denotes the complex conjugate. The frequency of the disturbance $\omega=-\alpha c$. Here, k denotes the harmonic index and n denotes the amplitude order. Substituting above expansion in the governing equations and extracting terms at various harmonic-amplitude orders (k,n) give rise to the amplitude equation (30), consequently the Landau constant $s^{(1)}$ is obtained.

For flows which are linearly stable, e.g., the plane Couette flow, Reynolds and Potter[14] suggested the equilibrium flow method. Here, instead of the linear flow, the nonlinear flow is assumed to be at the point of transition, such that $dA/dt=0$. In this formulation, the disturbance frequency is expanded in amplitude as

$$\omega = -\alpha c - \alpha \Lambda A^2 + \mathcal{O}(A^4), \tag{32}$$

where Λ is the correction to the linear wavespeed c. For nonlinear steady-state flow, the frequency is a real quantity, and we get the equilibrium amplitude as

$$A_e^2 = -\frac{c_i}{\Lambda_i}. \tag{33}$$

Since $c_i<0$ for linearly stable flows, a real-valued amplitude exists only if $\Lambda_i>0$, which means that the transition occurs through subcritical instability. The disturbances with amplitude larger than A_e grow with time. The threshold kinetic energy required for the finite amplitude instability is defined as

$$E = \frac{A_e^2}{2}\int_0^1 (\tilde{v}_y^2 + \tilde{v}_x^2)dy. \tag{34}$$

The equilibrium flow method has been used previously to estimate the threshold energy for subcritical instability in the plane Couette flow of Newtonian fluid.[5] The destabilizing effect of the nonlinearities in the plane Couette flow was further confirmed by Davey[50] using the above described method. In recent times, Morozov and Saarloos[15] employed this formulation to analyze the creeping flow of Maxwell fluid under shear. They also show that the inclusion of higher order terms in frequency expansion equation (32) does not significantly affect the stability behavior, which indicates that the expansion series (32) does converge for the flow they considered.

C. Numerical scheme

The most important part of this analysis is obtaining the eigenvalues of the linearized problem. Since by nature the classical Oldroyd-B model exhibits strong oscillations in polymeric stress in the cross-flow direction, the underresolved numerical scheme may show spurious instabilities, especially in the limit of high Weissenberg number[19] for the causes of spurious eigenvalues. In the present work, we convert the boundary value problem with unknown eigenvalues to initial value problem with unknown single eigenvalue using the shooting technique. The governing equations are integrated in the wall-normal direction using the Runge–Kutta method on an adaptive grid, and the unknown eigenvalue is calculated using the Newton–Raphson technique. This method provides a single eigenvalue in the vicinity of the initial guess value. As the grid size is adaptive, the eigenvalues are very accurate. This technique has been used successfully to calculate the wall mode eigenvalues for the shear flow past a flexible surface.[51,52]

While the dominant eigenvalue is calculated using the shooting method, we also use the Chebyshev-collocation technique to construct the entire eigenspectrum. The resolved eigenvalues of this spectrum are verified using the shooting method. The Chebyshev expansion to capture the variations in the Fourier modes in the cross-flow direction results in a generalized eigenvalue problem of the form

$$\mathcal{L}\tilde{\phi} = c\mathcal{M}\tilde{\phi}, \tag{35}$$

where $\mathcal{L}$ and $\mathcal{M}$ are the linear operators. The eigenspectrum in wavespeed c is obtained using the QZ algorithm. The eigenmode is stable if the imaginary part of wavespeed $c_i<0$, where as $c_i>0$, suggests linear instability. In later case, the neutral stability curve can be constructed by setting $c_i=0$.

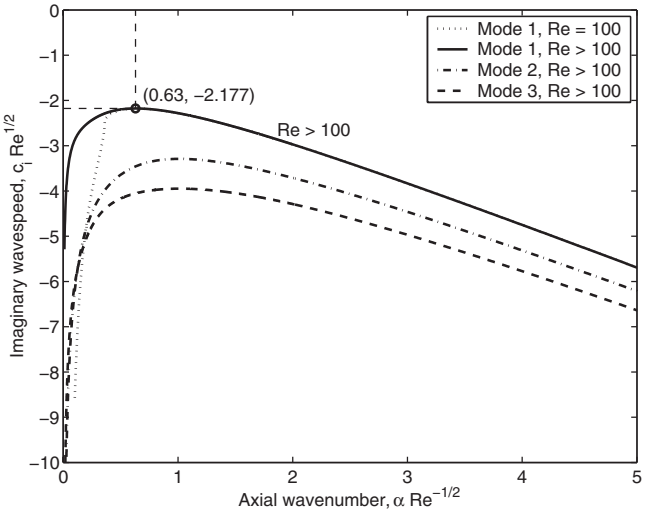

FIG. 1. Imaginary part of wavespeed against axial wavenumber for the Newtonian fluid. This plot holds for any Reynolds number Re>100.

IV. RESULTS AND DISCUSSION

A. Classical Oldroyd-B model

For a plane Couette flow of Newtonian fluid in the limit of high Reynolds number, the eigenmodes are confined to a thin layer near the walls within which the viscous and inertial stresses are comparable. This thin layer of thickness $O(\alpha\,\mathrm{Re})^{-1/3}$ is referred to as the wall layer and the eigenmodes the wall modes. The wall modes are believed to be linearly stable,[3] which means that the imaginary part of the wavespeed c_i is negative for all the modes. The damping rate is $-\alpha c_i$. The value of c_i reaches closest to zero for axial wavenumber $\alpha \sim \mathrm{Re}^{1/2}$ for $\mathrm{Re} \gg 1$.[3] Figure 1 plots $c_i\,\mathrm{Re}^{1/2}$ against $\alpha\,\mathrm{Re}^{-1/2}$ for the first three least stable wall modes. The curves for different Reynolds numbers collapse on to a single curve on the coordinates scaled with Re for $\mathrm{Re} \gg 1$. This plot is similar to the one shown in Ref. 3. For finite amplitude disturbances, the threshold kinetic energy for subcritical instability can be calculated. The kinetic energy, defined in Eq. (34), scales as $\mathrm{Re}^{-3/2}$ for $\mathrm{Re} \gg 1$. The threshold energy as a function of axial wavenumber is shown in Fig. 2 on the scaled coordinates. The disturbance kinetic energy is shown to be minimum for $\alpha \sim \mathrm{Re}^{1/2}$ for different values of

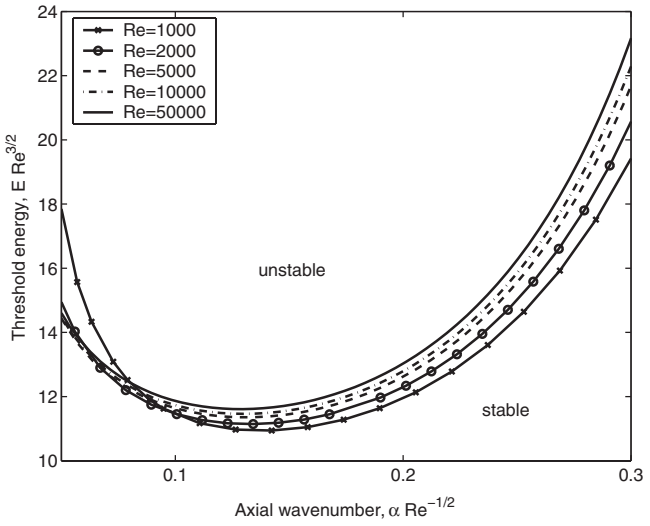

FIG. 2. Kinetic energy scaled with Reynolds number as a function of scaled axial wavenumber for the least stable Newtonian wall mode.

Reynolds number. Thus, the most dangerous disturbance has wavelength comparable to the thickness of the wall layer which is $O(\mathrm{Re}^{-1/2})$.[4,5]

The transition mechanism is believed to involve the 3D structures near the wall. Moreover, the full numerical simulations of 2D wall mode disturbances do not lead to self-sustaining turbulence.[6] Therefore, it is important to calculate the threshold energy for the 3D disturbances. Figure 3 shows the threshold energy as a function of axial wavenumber for different values of spanwise wavenumber α_z. Here, $\alpha_z=0$ indicates the 2D disturbance. The threshold energy for the oblique traveling waves in $x-z$ plane, that is, with $\alpha \neq \alpha_z \neq 0$, is found to be higher than the energy for axially traveling 2D disturbances. Although the simulations of Orszag and Kells[6] show that the initial disturbances must have a 3D disturbance in addition to a 2D disturbance, the amplitude of the 3D component is very small compared to the initial amplitude of a 2D component. Thus, the requirement of a 3D component appears to be to create 3D structures necessary for turbulence. However, for the onset of transition, the amplitude of a 2D component may provide the threshold criterion.

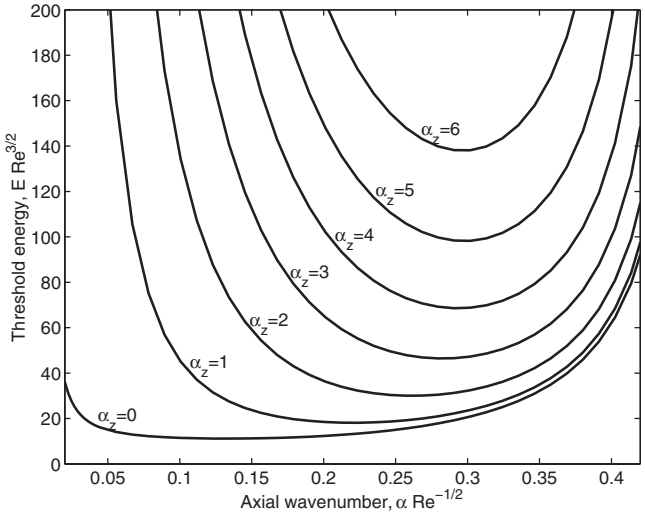

FIG. 3. Kinetic energy as a function of axial wavenumber for different values of spanwise wavenumber α_z. The 3D least stable Newtonian wall mode is analyzed for Re=2000.

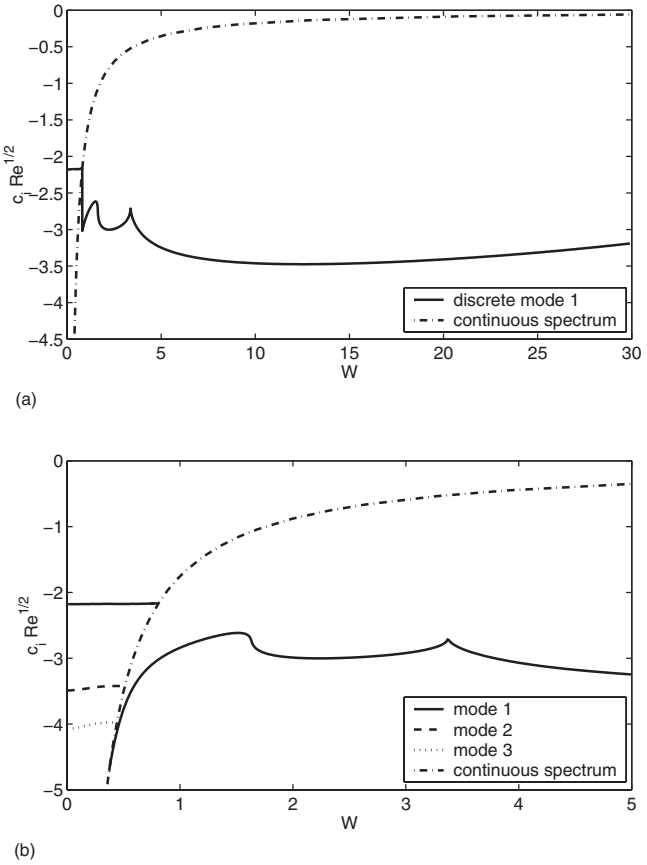

FIG. 4. The variation of the imaginary part of the wavespeed with flow Weissenberg number for the classical Oldroyd-B model for $\alpha=0.6\ \mathrm{Re}^{1/2}$ and $\beta=0.95$. (a) Mode 1 and a continuous spectrum are shown; (b) first three wall modes and a continuous spectrum are shown in the region with small Weissenberg number.

The effect of polymer additives on the wall mode disturbance is studied by numerical continuation of the wavespeed corresponding to the least stable Newtonian wall mode to viscoelastic fluid described by the classical Oldroyd-B equation (28). The variation in c_i with fluid Weissenberg number is shown in Fig. 4 for axial wavenumber $\alpha=0.6\ \mathrm{Re}^{1/2}$ and polymer viscosity parameter $\beta=0.95$. This figure shows a single curve on to which the plots for different Reynolds number collapse. For the classical Oldroyd-B fluid, there exist two continuous spectra of eigenvalues with wavespeeds $c=y-i/(\alpha W)$ and $c=y-i/(\alpha\beta W)$ attributed to the singularity in the perturbation equation (28). The second spectrum is a branch cut in eigenspectrum space across which the discrete eigenvalues appear and disappear upon changing parameters such as α, β, and W.[13] In Fig. 4(b), the first three wall modes are seen to merge with the continuous spectrum and disappear at $W<1$. On the other side with $W>1$, a new discrete eigenvalue emerges from the continuous spectrum. The variation in c_i for the least stable wall mode with wavenumber is shown in Fig. 5. This figure further demonstrates the

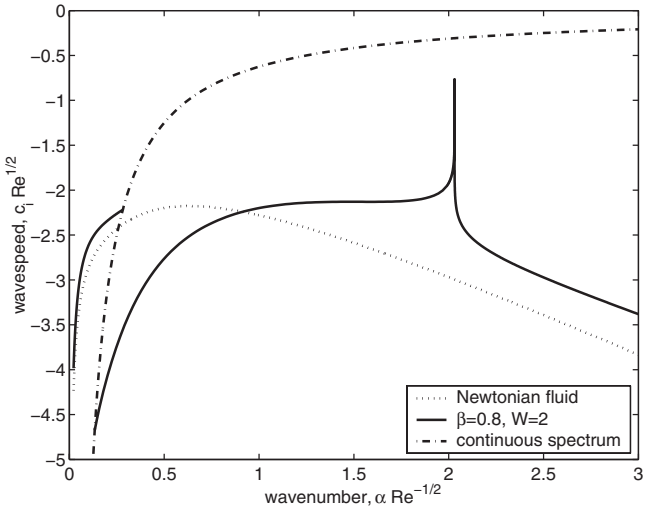

FIG. 5. Imaginary part of wavespeed against axial wavenumber for the classical Oldroyd-B fluid with $\beta=0.8$ and $W=2$. The curves for $\mathrm{Re}\gg 1$ collapse on to a single curve in the scaled coordinates.

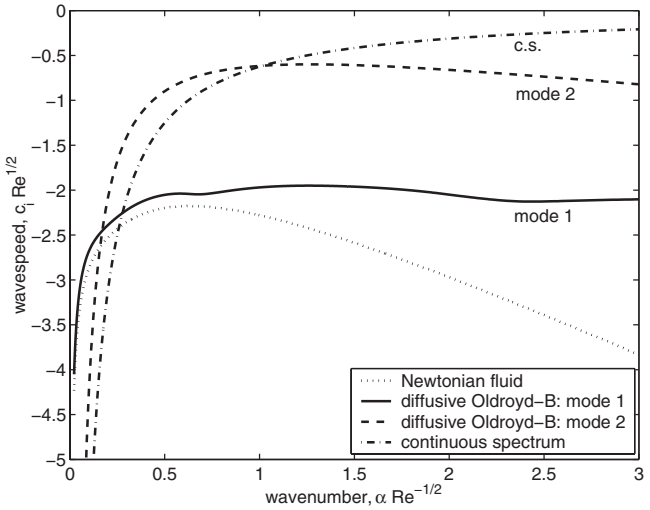

FIG. 7. Imaginary part of wavespeed against wavenumber for the diffusive Oldroyd-B model for $\mathrm{Re}=2000$, $\beta=0.8$, and $W=2$.

disappearance and the appearance of a discrete mode across the continuous spectrum. The least stable eigenvalue merges with the continuous spectrum and disappears before c_i approaches maximum. The mode that emerges out of the continuous spectrum, however, approaches close to the point of neutral stability with a decay rate much lower than that for the Newtonian fluid.

The weakly nonlinear stability of the classical Oldroyd-B fluid is analyzed by calculating Λ, the nonlinear contribution to the linear wavespeed, using the method of Reynolds and Potter.[14] The nonlinear flow undergoes transition only if the imaginary part Λ_i is positive. The calculations show that Λ_i is positive for a small wavenumber range before the polymeric wall mode merges with the continuous spectrum. Even before merging, the sign of Λ_i turns to negative. Figure 6 plots the threshold kinetic energy for a range of wavenumbers for which $\Lambda_i>0$, that is, the finite amplitude correction to the linear growth rate is destabilizing. Comparison with Fig. 2 indicates that this range of wavenumbers is narrow for the polymeric flow. The disturbance energy required for the subcritical instability is higher for the viscoelastic fluid than for the Newtonian fluid. Increasing the flow elasticity and addition of polymers tend to increase the threshold energy, as shown in Fig. 6 for increasing Weissenberg number and decreasing β, respectively. Thus, for a specified strength of wall mode disturbance, the addition of polymer molecules to the Newtonian fluid delays the transition to turbulence. Also seen for the figure is that the most dangerous disturbance is likely to have smaller wavenumber than that for the Newtonian flow.

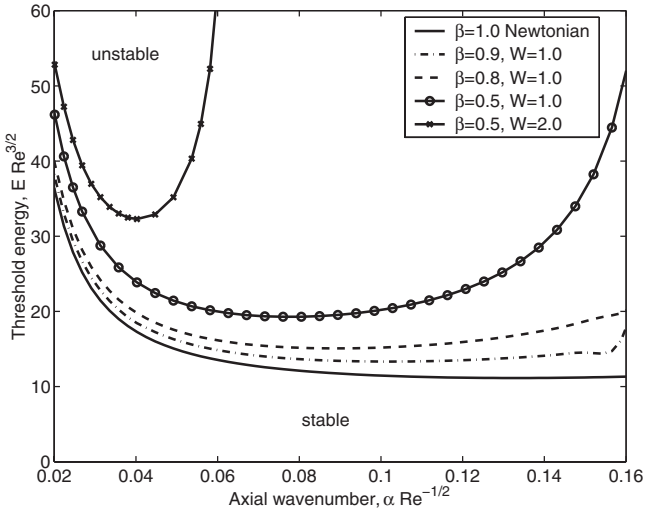

FIG. 6. Threshold kinetic energy as a function of scaled wavenumber for the least stable polymeric wall mode at $\mathrm{Re}=2000$. Curves for various Reynolds numbers fall closely but do not collapse on a single curve. For larger wavenumber the continuous spectrum interferes with the discrete wall mode.

B. Diffusive Oldroyd-B model

By addition of a diffusivity term in the conformation tensor equation (11), the continuous spectrum is destroyed and we witness only the discrete modes. As shown in Fig. 7, the wall mode, qualitatively similar to the Newtonian wall mode (indicated as mode 1), continues for large wavenumbers, even past the continuous spectrum line (existing for the classical Oldroyd-B model). This mode attains the least damping rate at $\alpha\sim 1.3\,\mathrm{Re}^{1/2}$ as against $\alpha\sim 0.63\,\mathrm{Re}^{1/2}$ for the Newtonian fluid. However, there exists another mode (indicated as mode 2) which becomes dominant to mode 1 at large wavenumber. This mode is qualitatively different from the Newtonian wall mode, since it does not continue to the Newtonian wall mode as β approaches unity. Figure 8 shows the eigenspectrum for both the classical Oldroyd-B model as well as the diffusive Oldroyd-B model. Upon incorporation of stress diffusivity, the destruction of the continuous spectra present in the classical Oldroyd-B model is clearly visible. Also, the dominance of mode 2 over mode 1 is also shown in Fig. 8(d). The Chebyshev expansion with number of collocation points $N=120$ is used to construct the eigenspectra which remained unchanged upon increasing the resolution. We have used the no-flux boundary condition for the confor-

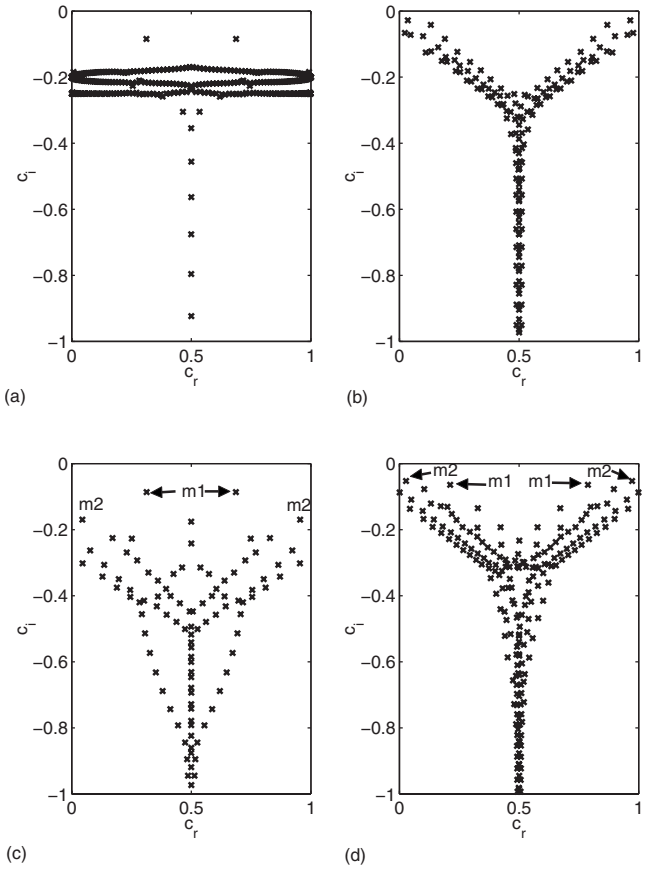

FIG. 8. Eigenspectrum for the classical and diffusive Oldroyd-B models. The no-flux of polymer conformation condition is used for the diffusive Oldroyd-B model. Parameters are Re=2000, β=0.8, W=5. (a) Classical Oldroyd-B: α=1; (b) diffusive Oldroyd-B: α=10, Pe=10^3; (c) diffusive Oldroyd-B: α=1, Pe=10^4; (d) diffusive Oldroyd-B: α=3, Pe=10^4. Here, "m1" and "m2," respectively, represent the modes 1 and 2 of Fig. 7.

mation tensor equation to generate the results for the diffusive Oldroyd-B model. However, we find the results to be qualitatively similar for the other type of boundary condition, that is, enforcing the classical Oldroyd-B equation at the walls. The typical structure of eigenfunctions corresponding

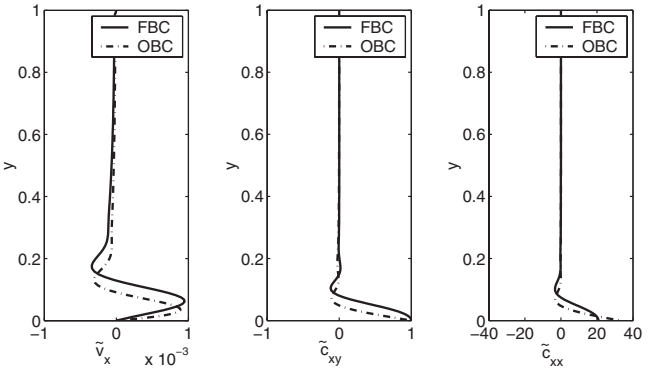

FIG. 9. The structure of eigenfunctions and its sensitivity to the type of boundary condition for the stable diffusion mode. The parameters are Re=2000, α=3, β=0.8, W=5, and Pe=10^4. Real parts of the disturbances $\tilde{v}_y(y)$, $\tilde{c}_{xy}(y)$, and $\tilde{c}_{xx}(y)$ are plotted. Here, "FBC" means the no-flux boundary condition for conformation tensor and "OBC" indicates the use of classical Oldroyd-B equation at the walls.

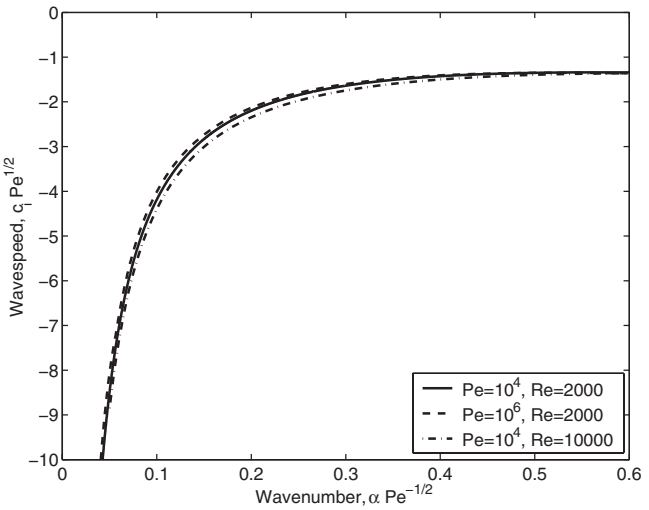

FIG. 10. Imaginary part of wavespeed against wavenumber, both scaled with Péclet number, for the diffusive Oldroyd-B model for β=0.8 and W=2.

to the diffusion mode is shown in Fig. 9 for both the types of boundary conditions. The eigenfunctions are obtained by using the normalization condition $\tilde{c}_{xy}|_{y=0}=1$. Only the real parts of the disturbances $\tilde{v}_x$, $\tilde{c}_{xy}$, and $\tilde{c}_{xx}$ are shown. As seen, the disturbances are confined to a narrow region near the wall.

Since mode 2 is found to be the slowest decaying mode for wavenumber proportional to $\mathrm{Re}^{1/2}$, its origin needs to be examined. To start with, the effect of Péclet number on this mode is studied. We find that the imaginary part of wavespeed corresponding to this mode decreases proportional to $\mathrm{Pe}^{-1/2}$. Figure 10 shows the variation in c_i with wavenumber. The curves for Pe=10^4 and Pe=10^6 fall on a single curve when c_i is scaled with $\mathrm{Pe}^{-1/2}$ and wavenumber with $\mathrm{Pe}^{1/2}$. This scaling of wavespeed can be obtained by comparing the orders of various terms in the conformation tensor governing equation (11). The diffusion term is comparable to the convective and the relaxation terms in a narrow region of thickness $l \sim O(W/\mathrm{Pe})^{1/2}$. This region is the diffusion layer for the conformation tensor, hence we refer to this mode as "diffusion mode." For a creeping flow of UCM fluid, Gorodtsov and Leonov[10] found two discrete eigenmodes (GL modes), known in literature as the elastic modes. A pair of least stable diffusion mode is believed to be qualitatively similar to the GL modes modified by the diffusion term and fluid inertia. For low wavenumber case with $\alpha \sim O(1)$, the diffusion mode decays much faster than the wall mode (see Fig. 7), and hence can be ignored. However, for large wavenumber disturbances, which is the focus of present analysis, the diffusion mode becomes less stable than the wall modes. For $\mathrm{Pe} \gg \mathrm{Re}$, the thickness of diffusion layer l is smaller than the length scale of wall modes, which is $\delta \sim (\alpha\ \mathrm{Re})^{-1/3}$. For this case, in the fluid momentum equation (9), the viscous stresses balance with the elastic polymeric stresses within the diffusion layer and the inertial terms become subdominant in this region. Consequently, the flow Reynolds number does not influence the eigenmode appreciably, which was evident from Fig. 10, wherein the values of c_i for Re=2000 and 10 000 are seen to be very close.

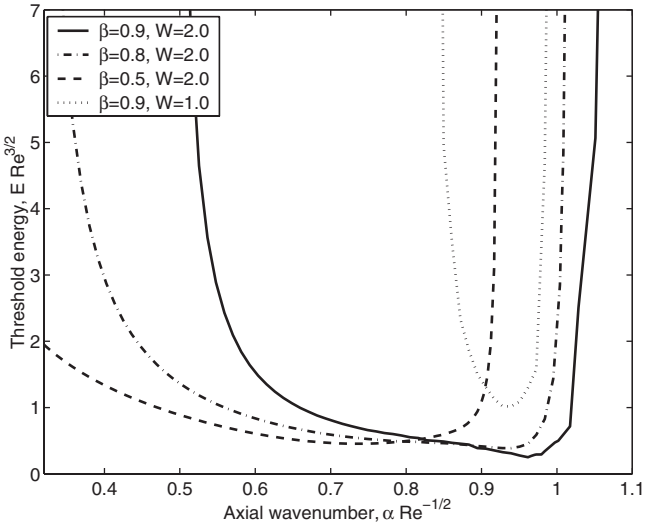

FIG. 11. Diffusive Oldroyd-B model: The threshold energy for Re=2000, $W=2$, Pe=10^4, and different values of β.

The finite amplitude stability was analyzed for the diffusion mode, and it is found that the nonlinear correction Λ_i is positive for a range of wavenumber much wider than for the wall modes. Figure 11 shows the threshold energy as a function of wavenumber for a typical case of Re=2000 and Pe=10^4. A comparison with Fig. 6 for the wall mode shows that the threshold energy for the diffusive Oldroyd-B fluid is lower in magnitude than that for the classical Oldroyd-B fluid. As shown in Fig. 11, the threshold energy attains a minimum for $\alpha \sim \mathrm{Re}^{1/2}$ for the given set of parameters. Also seen from the figure is that the threshold kinetic energy is lower for fluid with higher Weissenberg number.

C. Nonhomogeneous polymer solution model

A more rigorous model involving the diffusion effects of the polymer chains should account for the local nonhomogeneity of polymer concentration. The stability of base flow profiles for the nonhomogeneous Oldroyd-B model is analyzed for two kinds of boundary condition for the conformation tensor: (1) enforce the governing equation for conformation tensor [Eq. (14)] with Pe$\rightarrow\infty$ at the walls; and (2) zero flux of conformation tensor ($d_y\mathbf{C}=0$) across the walls. The steady-state solution for both these boundary conditions is identical and is same as that for the previous two models, meaning the polymer conformation as well as the concentration is uniform across the channel. For the first kind of boundary condition, Fig. 12(a) shows the effect of fluid elasticity on the imaginary part of wavespeed c_i for the least stable mode. As c_i changes sign, the base profile becomes unstable when Weissenberg number exceeds a certain transition value W_t given by $c_i=0$. The transition Weissenberg number is higher for larger values of Péclet number and for Pe$\geq 10^6$, the instability ceases to exist. Figure 12(b) shows the neutral stability curve in W_t-α plane. The minimum on this curve gives the critical point with critical Weissenberg numbers W_c and α_c. For the first kind of boundary condition, the critical point lies on the large wavenumber plateau. For the no-flux condition, the stability behavior is shown in

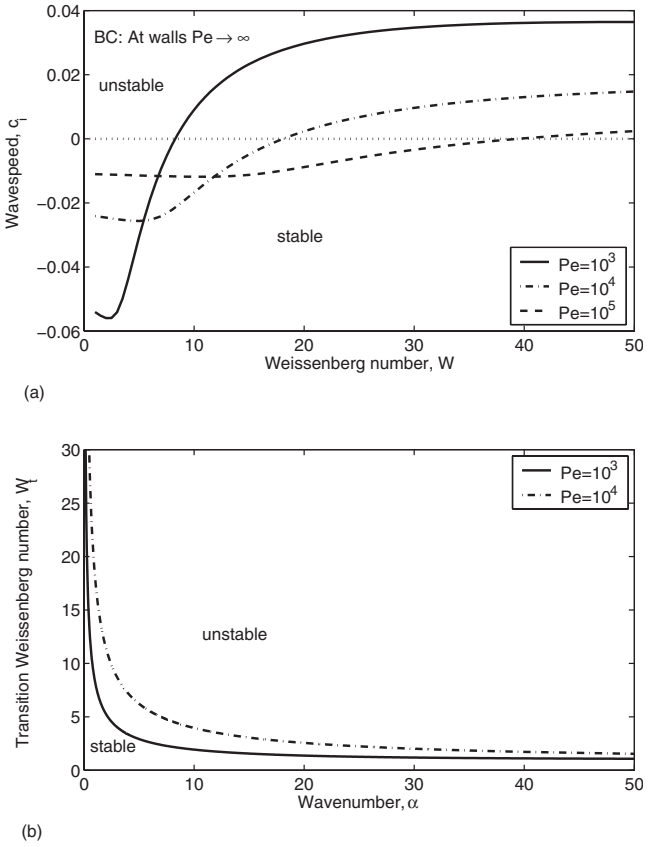

FIG. 12. Stability behavior for the nonhomogeneous Oldroyd-B model using conformation equation with Pe$\rightarrow\infty$ as the boundary condition. The parameters are Re=2000, $\alpha=1$, and $\beta=0.95$. (a) Variation in c_i with Weissenberg number; (b) the transition Weissenberg number as a function of disturbance wavenumber.

Fig. 13. Here also, the instability is observed for $W>W_t$. For this case, the transition value W_t attains a minimum value for a finite wavenumber, as shown in Fig. 13(b). The critical Weissenberg number is lowered by adding more polymer molecules to the solution, i.e., by reducing β.

The unstable mode for the nonhomogeneous solutions is the concentration mode giving rise to the demixing due to strong concentration fluctuations near the walls. By demixing we mean that the uniform profile for the polymer number density tends to become unstable beyond the point of transition. Figure 14 shows a typical eigenspectrum showing a pair of unstable eigenmodes traveling downstream at a speed close to the base flow velocity near the walls. The first few least stable eigenvalues are listed in Table I for both kinds of boundary condition for polymer conformation. The concentration mode instability is governed mainly by the equation for polymer number density [Eq. (16)]. In this equation, the balance between the Fickian diffusion of polymer concentration and stress-induced migration governs the evolution of a disturbance in concentration field. While the Fickian diffusion gives stable eigenvalues, instability is caused by the stress-induced migration effect. The stable eigenvalues for molecular diffusion are modified by the migration term to result in unstable eigenvalue, we refer to as the concentration mode. Identifying the origin of other modes in the eigenspectrum is not a straightforward continuation of other existing

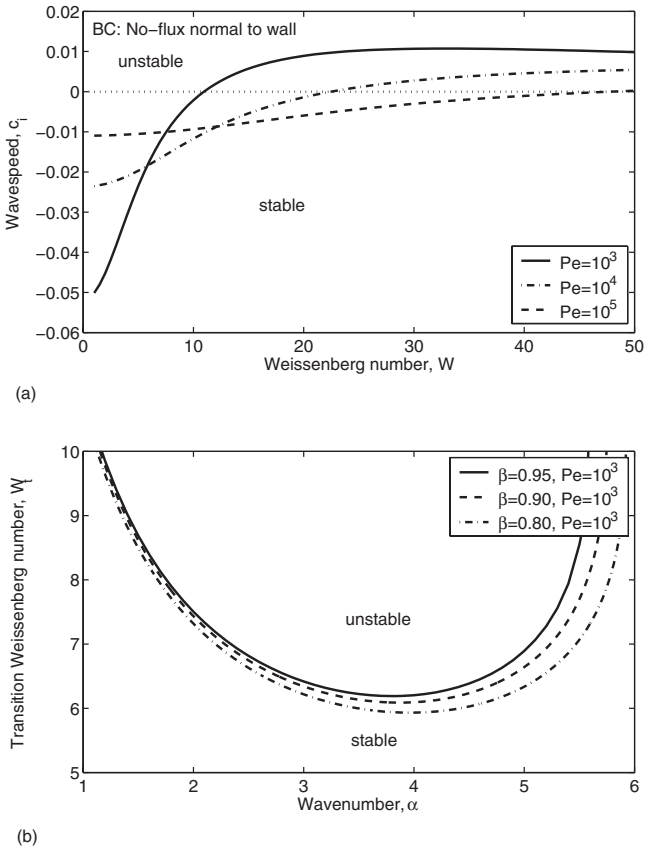

FIG. 13. Stability behavior for the nonhomogeneous Oldroyd-B model using zero conformation flux across walls as the boundary condition. The parameters are Re=2000 and $\alpha=1$. (a) Variation in c_i with Weissenberg number for $\beta=0.95$; (b) the transition Weissenberg number as a function of disturbance wavenumber for different β.

modes for the homogeneous case. However, based on the analogy with the diffusion mode discussed in Sec. IV B for the diffusive Oldroyd-B model, we can term the four pairs of modes after the concentration modes, as the diffusion modes. These modes are similar to the diffusion mode discussed in Sec. III, although modified by the presence of concentration fluctuations. The Newtonian wall mode modified by the flow elasticity is found to be decaying faster than the other kinds of modes. The eigenfunctions for all kinds of modes are confined to a thin region near the walls. The typical structure of eigenfunctions corresponding to the concentration mode is shown in Fig. 15 for both the types of boundary conditions. The eigenfunctions are obtained by using the normalization condition $\tilde{C}_{xy}|_{y=0}=1$. Only the real parts of the disturbances $\tilde{n}$, $\tilde{C}_{xy}$, and $\tilde{C}_{xx}$ are shown. The structure of the eigenfunctions is apparently similar for both kinds of boundary conditions.

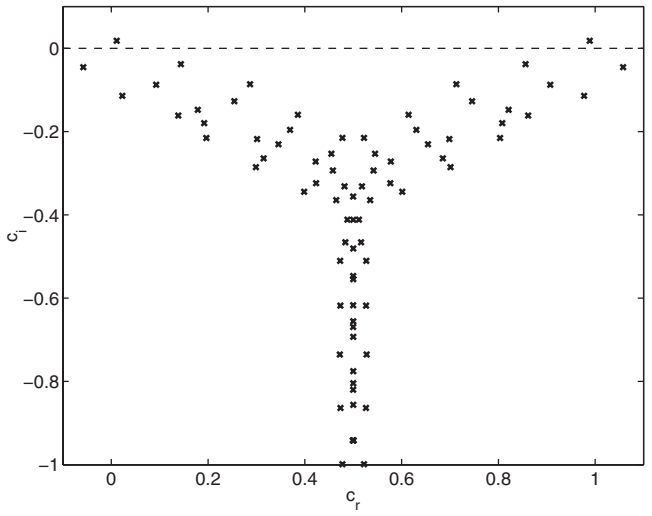

FIG. 14. Eigenspectrum for the nonhomogeneous polymer model: Re=2000, $\alpha=2$, $\beta=0.8$, $W=10$, and Pe=10^3. Conformation equation with Pe$\to\infty$ is used at the walls.

The instability due to the concentration fluctuations was found earlier by Black and Graham[31] for the creeping flow of UCM fluid ($\beta=0$). For their case, the concentration mode was found to be stable for a set of parameters studied. However, the mode becomes unstable upon incorporating slip at the walls. We continue the unstable concentration mode discussed above for the dilute solutions to the UCM fluid by reducing the solvent viscosity parameter β to zero. Figure 16 shows the variation of c_i with β using the no-flux condition for polymer conformation, a condition used by Ref. 31. The unstable mode stabilizes when β is reduced to zero, which is consistent with the observation of Black and Graham.[31] It should be noted here that the fluid Reynolds number does not affect the concentration mode appreciably. Although the concentration equation (16) is coupled with the fluid momentum balance equation (12), the coupling, however, is found to be weak.

The weakly nonlinear analysis is performed to examine the nature of bifurcation to finite amplitude states at the point of linear instability. Figure 17 shows the variation in disturbance amplitude in the vicinity of transition Weissenberg number. For the boundary condition in which the conformation equation with Pe$\to\infty$ being applied at the walls, the nonlinear effects are further destabilizing, resulting in a subcritical instability at Weissenberg number lower than W_t [see Fig. 17(a)]. On the contrary, the nonlinear contribution is stabilizing for the no-flux condition for polymer conformation at the walls, leading to supercritical stability for $W>W_c$ [see Fig. 17(b)].

Before closing the analysis in this chapter, we briefly analyze a variant of nonhomogeneous polymer model used above. Following the derivation by Mavrantzas and Beris[25] using the Hamiltonian for two fluid phases, the polymer conformation equation explicitly includes the two-fluid effects. In this approach, the polymer conformation is given by

$$\frac{\partial \mathbf{C}}{\partial t} + \nabla \cdot (\mathbf{v}^p \mathbf{C}) - \mathbf{C} \cdot \nabla \mathbf{v}^p - (\nabla \mathbf{v}^p)^T \cdot \mathbf{C} = -\frac{(\mathbf{C} - n\mathbf{I})}{W} + \frac{1}{\mathrm{Pe}} \nabla^2 \mathbf{C}. \tag{36}$$

Here the upper convected derivative is based on the polymer phase velocity $\mathbf{v}^p=\mathbf{v}+(1-\phi)\Delta\mathbf{v}$, where ϕ is the polymer mass fraction and $\Delta\mathbf{v}$ is the differential velocity. For dilute solutions $\phi \ll 1$ and the differential velocity is proportional to the mass flux, $\Delta\mathbf{v}=\mathbf{J}/n$. Here the total flux of polymer mol-

TABLE I. The list of first few least stable eigenvalues for the two kinds of boundary conditions for the conformation tensor. The parameters are: Re=2000, $\alpha=1$, $\beta=0.95$, and Pe=10^4.

Classical Oldroyd-B equation at walls $W=20$		No-flux boundary condition $W=25$
Eigenvalue c	Mode type	Eigenvalue c
0.010 670 377+0.002 331 849	Concentration modes	0.041 615 254+0.001 117 870
0.989 335 130+0.002 329 887		0.958 382 817+0.001 116 054
0.082 587 029−0.028 864 934	Diffusion modes	0.135 027 773−0.049 738 761
0.917 413 569−0.028 869 094		0.864 969 057−0.049 738 511
−0.038 641 202−0.045 360 697		−0.005 504 068−0.056 119 828
1.038 638 070−0.045 353 810		1.005 505 420−0.056 117 066
0.059 217 404−0.066 472 986		0.086 908 934−0.061 028 747
0.940 809 903−0.066 469 833		0.913 081 312−0.061 029 092
0.168 990 859−0.072 437 195		0.198 570 158−0.090 949 441
0.831 008 778−0.072 433 318		0.801 430 487−0.090 942 489
0.311 007 525−0.092 397 516	Wall mode 1	0.311 142 431−0.093 444 197
0.689 008 742−0.092 405 826		0.688 886 636−0.093 402 577
0.009 777 403−0.092 938 728	Diffusion modes	0.043 075 445−0.110 107 065
0.990 215 279−0.092 934 440		0.956 926 845−0.110 109 909
0.093 187 589−0.103 190 160		0.099 265 468−0.113 790 868
0.906 789 166−0.103 190 784		0.900 724 373−0.113 804 804
0.227 470 563−0.109 251 509	Concentration modes	0.253 584 826−0.124 958 837
0.772 524 904−0.109 253 305		0.746 449 179−0.124 988 079
⋯		⋯
⋯		⋯
0.499 902 225−0.193 338 078	Wall mode 2	0.499 984 729−0.193 417 592

ecules **J** is given by Eq. (19). Thus, the expression of the polymer phase velocity is

$$\mathbf{v}^p = \mathbf{v} + \frac{\mathbf{J}}{n}, \tag{37}$$

where **v** is the fluid velocity field. This two-phase model was used to study the migration and the instability in Taylor–Couette flow.[27] Recently, the direct numerical simulation of turbulent boundary layer flow was carried out for the nonhomogeneous polymeric flow described by the above discussed two-fluid model.[53] For the base state of our interest, the polymer flux **J** is zero and $\mathbf{v}^p=\mathbf{v}$. However, the strongly varying

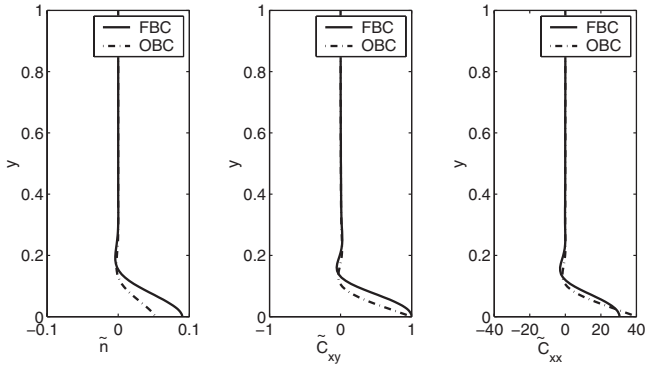

FIG. 15. The structure of eigenfunctions and its sensitivity to the type of boundary condition for the unstable concentration mode. The parameters are Re=2000, $\alpha=1$, $\beta=0.95$, $W=25$, and Pe=10^4. Typical disturbances $\tilde{n}(y)$, $\tilde{C}_{xy}(y)$, and $\tilde{C}_{xx}(y)$ are plotted. Here, "FBC" means the no-flux boundary condition for conformation tensor and "OBC" indicates the use of classical Oldroyd-B equation at the walls.

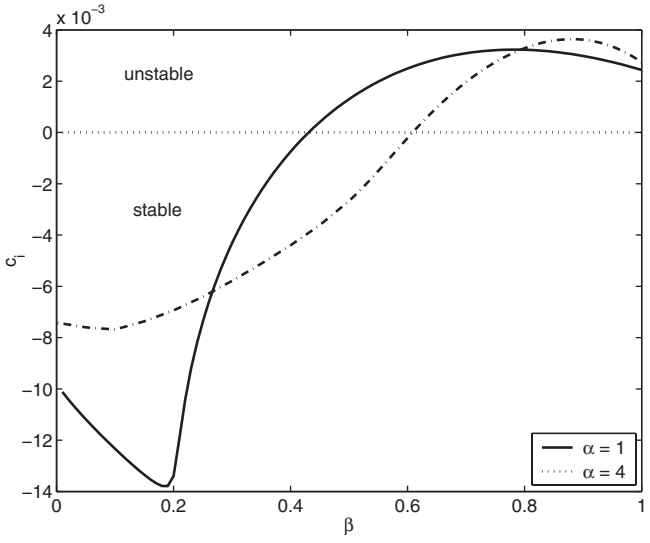

FIG. 16. Imaginary part of wavespeed as a function of solvent viscosity parameter β for the nonhomogeneous Oldroyd-B model. Parameters: Re=2000, $W=30$, and Pe=10^4. The no-flux condition is used for the polymer conformation tensor at the walls.

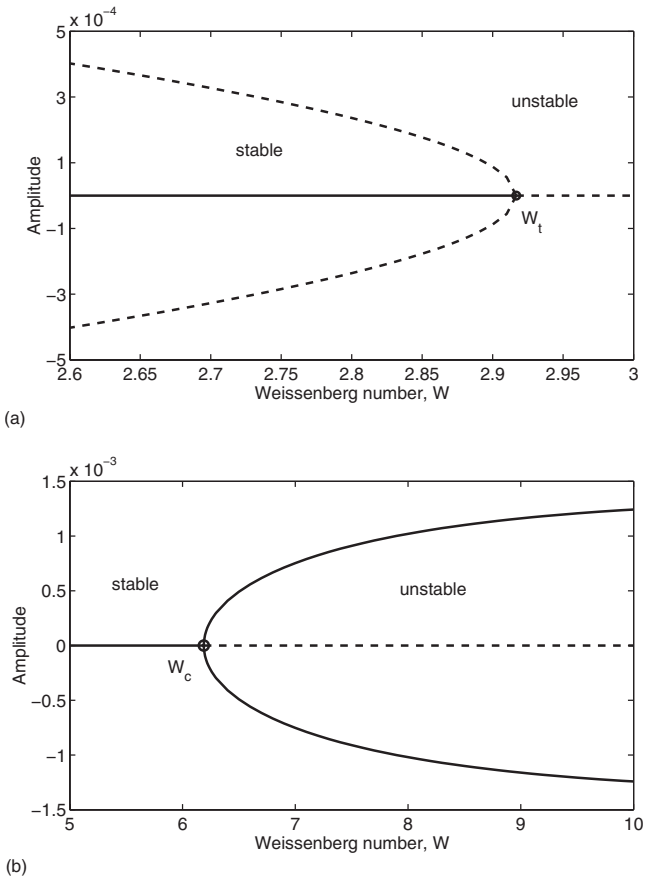

FIG. 17. Disturbance amplitude as a function of Weissenberg number, the transition parameter, in the vicinity of the transition point. (a) Re=2000, α=3.8, β=0.95, and Pe=10^3. BC: Conformation equation with Pe$\to\infty$; (b) Re=2000, α=5.0, β=0.95, and Pe=10^3. BC: No-flux across walls for the conformation tensor.

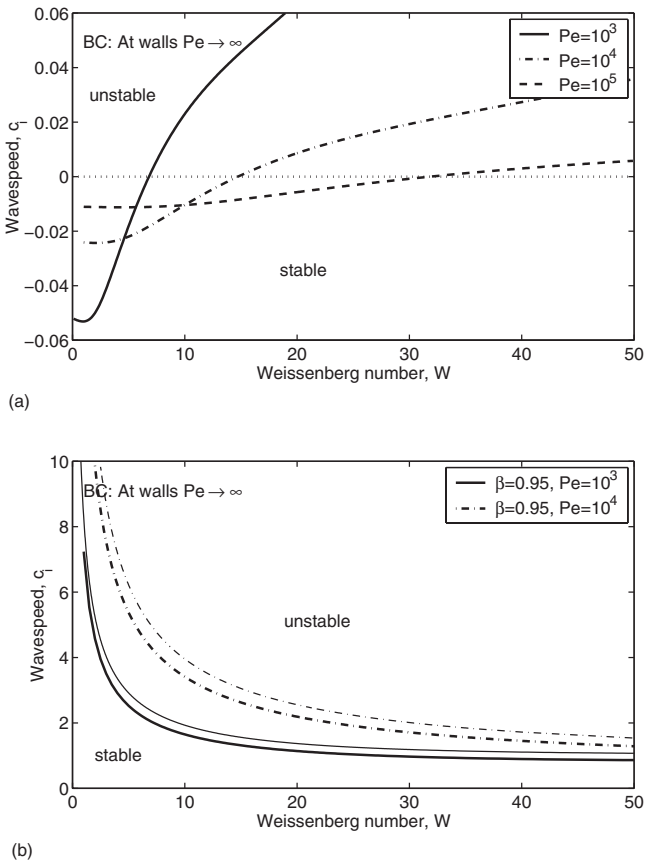

FIG. 18. Stability behavior for the nonhomogeneous Oldroyd-B model with two-fluid effects using the conformation equation with Pe$\to\infty$ as boundary condition. (a) Re=2000, α=1, and β=0.95; (b) Re=2000. Here, the thin lines indicate respective curves for the model without two-fluid effects [taken from Fig. 12(b)].

flux disturbance may influence the polymer dumbbell velocity and consequently the stability behavior. We, therefore, examine the stability of nonhomogeneous polymeric flow using Eq. (36) for conformation tensor. Figure 18 shows the effect of Weissenberg number on c_i applying Eq. (36) with Pe$\to\infty$ at the walls. Like for the earlier case, the instability is observed. We find the transition Weissenberg number W_t to be marginally smaller than its value for the case $\mathbf{v}^p=\mathbf{v}$ shown in the respective Fig. 12.

V. CONCLUSIONS

The nature of interaction of macromolecules, capable of extracting energy from the surrounding and storing it in the form of elastic energy, with the hydrodynamics, which drives the polymeric chains away from equilibrium, has been studied for many years. In the present work, with the focus on the on-set of transition, we carried out the stability analysis of dilute polymeric flow. Both the linear and the finite amplitude stability were analyzed for 2D disturbances in a plane Couette flow. In the widely studied problem of plane Poiseuille flow, the axial wavenumber of interest is $O(1)$.[17] However, following the earlier finding that the most dangerous finite amplitude disturbance for the Newtonian wall mode has wavelength comparable to the thickness of wall layer,[4] our analysis is focused on disturbances with wavenumber $\alpha\sim \mathrm{Re}^{1/2}$, for which the thickness of wall layer is $O(\mathrm{Re}^{-1/2})$. For these disturbances the finite amplitude stability of polymeric wall mode is examined first using the classical Oldroyd-B model for the viscoelastic fluid. We find that the threshold kinetic energy necessary for subcritical transition in polymeric flow is higher than that for the Newtonian flow and the energy is proportional to $\mathrm{Re}^{-3/2}$ for Re$\gg$1, a scaling similar to the Newtonian fluids.

The presence of the continuous spectra in the classical Oldroyd-B model prevents the continuation of the wall mode eigenvalue to large Weissenberg number. One of the spectra, which is a branch cut in eigenvalue space, does not allow a continuous evolution of the discrete eigenvalues. Following a common practice, an artificial diffusivity is added to the Oldroyd-B model. As known already, this modification destroys the spectra and allows continuous evolution of eigenvalues. However, the diffusive equation for the polymer conformation gives rise to other discrete modes, referred to as the diffusion modes. While the diffusion modes are subdominant to the wall modes (i.e., decay faster than the wall modes) for wavenumber $O(1)$, few of them becomes the least stable modes for large wavenumbers. The diffusion modes scale with Péclet number as $c_i\sim \mathrm{Pe}^{-1/2}$. From the weakly nonlinear analysis we observe that the threshold ki-

netic energy is small compared to that for the Newtonian fluids.

Another variant of the Oldroyd-B model, which accounts for nonhomogeneous polymer number density, has also been analyzed for stability of the base profiles. The concentration fluctuations due to the coupled distribution of polymer mass and stress are found to destabilize the concentration mode which becomes unstable when the fluid Weissenberg number exceeds a transition value W_t. The instability was observed for two kinds of boundary conditions tested in the present study, i.e., applying the Oldroyd-B equation for polymer conformation with $\mathrm{Pe}\to\infty$ at the wall, and applying no-flux of conformation across the walls. This instability tends to transform the uniform concentration profile in the base flow into a nonuniform distribution near the walls, leading to demixing.

A comment on physical realizability of the instability seems worth making at this point. Usually the artificial diffusivity term is added only to regularize the singular eigenfunctions and it should be small enough not to influence the flow. However, Péclet numbers of the order of 10^4-10^5 or even smaller are employed in numerical simulations to capture the polymer-induced drag reduction. Therefore, the present analysis covers the range $\mathrm{Pe}=10^3-10^5$. As mentioned in Sec. IV C, the linear instability driven by the concentration mode does not exist for $\mathrm{Pe}\geq 10^6$. Hence, it remains to be seen if this instability can be observed in practice.

[1] A. E. Gill, "On the behaviour of small disturbances to Poiseuille flow in a circular pipe," J. Fluid Mech. **21**, 145 (1965).
[2] E. Gill, "A mechanism for instability of plane Couette flow and of Poiseuille flow in a pipe," J. Fluid Mech. **21**, 503 (1965).
[3] A. Davey, "On the stability of plane Couette flow to infinitesimal disturbances," J. Fluid Mech. **57**, 369 (1973).
[4] A. Davey and H. P. F. Nguyen, "Finite amplitude stability of pipe flow," J. Fluid Mech. **45**, 701 (1971).
[5] T. Coffee, "Finite amplitude instability of plane Couette flow," J. Fluid Mech. **83**, 401 (1977).
[6] S. A. Orszag and L. C. Kells, "Transition to turbulence in plane Poiseuille and plane Couette flow," J. Fluid Mech. **96**, 159 (1980).
[7] M. Nagata, "Three-dimensional finite amplitude solutions in plane Couette flow: Bifurcation from infinity," J. Fluid Mech. **217**, 519 (1990).
[8] M. Nagata, "Three-dimensional traveling-wave solutions in plane Couette flow," Phys. Rev. E **55**, 2023 (1997).
[9] U. Ehrenstein, M. Nagata, and F. Rincon, "Three-dimensional nonlinear plane Poiseuille-Couette flow homotopy revisited," Phys. Fluids **20**, 064103 (2008).
[10] V. A. Gorodtsov and A. I. Leonov, "On a linear instability of a plane parallel Couette flow of viscoelastic fluid," J. Appl. Math. Mech. **31**, 310 (1967).
[11] M. Renardy, "Rigorous stability proof for plane Couette flow of an upper convected Maxwell fluid at zero Reynolds number," J. Non-Newtonian Fluid Mech. **11**, 511 (1992).
[12] M. Renardy and Y. Renardy, "Linear stability of plane Couette flow of an upper convected Maxwell fluid," J. Non-Newtonian Fluid Mech. **22**, 23 (1986).
[13] H. J. Wilson, M. Renardy, and Y. Renardy, "Structure of the spectrum in zero Reynolds number shear flow of the UCM and Oldroyd-B liquids," J. Non-Newtonian Fluid Mech. **80**, 251 (1999).
[14] W. C. Reynolds and M. C. Potter, "Finite amplitude instability of parallel shear flows," J. Fluid Mech. **27**, 465 (1967).
[15] A. N. Morozov and W. Saarloos, "Subcritical finite-amplitude solutions for plane Couette flow of viscoelastic fluids," Phys. Rev. Lett. **95**, 024501 (2005).
[16] R. Sureshkumar and A. N. Beris, "Linear stability analysis of viscoelastic Poiseuille flow using an Arnoldi-based orthogonalization algorithm," J. Non-Newtonian Fluid Mech. **56**, 151 (1995).
[17] B. Sadanandan and R. Sureshkumar, "Viscoelastic effects on the stability of wall-bounded shear flows," Phys. Fluids **14**, 41 (2002).
[18] R. Sureshkumar, "Numerical observations on the continuous spectrum of the linearized viscoelastic operator in shear dominated complex flows," J. Non-Newtonian Fluid Mech. **94**, 205 (2000).
[19] R. Kupferman, "On the linear stability of plane Couette flow for an Oldroyd-B fluid and its numerical approximation," J. Non-Newtonian Fluid Mech. **127**, 169 (2005).
[20] A. W. El-Kareh and L. G. Leal, "Existence of solutions for all Deborah numbers for a non-Newtonian model modified to include diffusion," J. Non-Newtonian Fluid Mech. **33**, 257 (1989).
[21] R. Sureshkumar and A. N. Beris, "Effect of artificial stress diffusivity on the stability of numerical calculations and the flow dynamics of time-dependent viscoelastic flows," J. Non-Newtonian Fluid Mech. **60**, 53 (1995).
[22] R. Sureshkumar, A. N. Beris, and R. A. Handler, "Direct numerical simulation of the turbulent channel flow of a polymer solution," Phys. Fluids **9**, 743 (1997).
[23] A. V. Bhave, R. C. Armstrong, and R. A. Brown, "Kinetic theory and rheology of dilute, non-homogeneous polymer solutions," Chem. Phys. **14**, 2988 (1991).
[24] H. C. Öttinger, "Incorporation of polymer diffusivity and migration into constitutive equations," Rheol. Acta **31**, 14 (1992).
[25] V. G. Mavrantzas and A. N. Beris, "Modeling of the rheology and flow-induced concentration changes in polymer solutions," Phys. Rev. Lett. **69**, 273 (1992).
[26] A. N. Beris and V. G. Mavrantzas, "On the compatibility between various macroscopic formalisms for the concentration and flow of dilute polymer solutions," J. Rheol. **38**, 1235 (1994).
[27] M. V. Apostolakis, V. G. Mavrantzas, and A. N. Beris, "Stress gradient-induced migration effects in the Taylor-Couette flow of a dilute polymer solutions," J. Non-Newtonian Fluid Mech. **102**, 409 (2002).
[28] R. H. Shafer, N. Laiken, and B. H. Zimm, "Radial migration of DNA molecules in cylindrical flow. Part I. Theory of the free–draining model," Biophys. Chem. **2**, 180 (1974).
[29] M. J. MacDonald and S. J. Muller, "Experimental study of shear-induced migration of polymers in dilute solutions," J. Rheol. **40**, 259 (1996).
[30] W. B. Black, "Wall slip and boundary effects in polymer shear flows," Ph.D. thesis, University of Wisconsin, Madison, 2000.
[31] W. B. Black and M. D. Graham, "Slip, concentration fluctuations, and flow instability in sheared polymer solutions," Macromolecules **34**, 5731 (2001).
[32] L. P. Cook and L. F. Rossi, "Slippage and migration in models of dilute wormlike micellar solutions and polymeric fluids," J. Non-Newtonian Fluid Mech. **116**, 347 (2004).
[33] H. Krämer and B. A. Wolf, "Large fluctuations in polymer solutions under shear," Makromol. Chem., Rapid Commun. **6**, 21 (1985).
[34] H. Gerard, J. T. Cabral, and J. S. Higgins, "Flow-induced enhancement of concentration fluctuations in polymer mixtures," Philos. Trans. R. Soc. London, Ser. A **361**, 767 (2003).
[35] C. Rangel-Nafaile, A. B. Metzner, and K. F. Wissbrun, "Large fluctuations in polymer solutions under shear," Macromolecules **17**, 1187 (1984).
[36] R. G. Larson, "Flow-induced mixing, demixing, and phase transitions in polymeric fluids," Rheol. Acta **31**, 497 (1992).
[37] C. C. Han, Y. Yonghua, Z. Ruoyu, and K. H. Erik, "Effect of shear flow on multi-component polymer mixtures," Polymer **47**, 3271 (2006).
[38] E. Helfand and G. H. Fredrickson, "Large fluctuations in polymer solutions under shear," Phys. Rev. Lett. **62**, 2468 (1989).
[39] A. Onuki, "Elastic effects in the phase transition of polymer solutions under shear flow," Phys. Rev. Lett. **62**, 2472 (1989).
[40] A. Onuki, "Shear-induced phase separation in polymer solutions," J. Phys. Soc. Jpn. **59**, 3427 (1990).
[41] M. Doi and A. Onuki, "Dynamic coupling between stress and composition in polymer solutions and blends," J. Phys. II **2**, 1631 (1992).
[42] S. T. Milner, "Hydrodynamics of semidilute polymer solutions," Phys. Rev. Lett. **66**, 1477 (1991).
[43] M. Minale, "Stress induced demixing of a polymer solution: Mechanic interpretation with a suitable formulation of the two-fluid theory," Macromolecules **41**, 4471 (2008).
[44] P. D. Olmsted and C.-Y. D. Lu, "Phase coexistence of complex fluids in shear flow," Faraday Discuss. **112**, 183 (1999).
[45] S. M. Fielding and P. D. Olmsted, "Early stage kinetics in a unified model

of shear-induced demixing and mechanical shear banding instabilities," Phys. Rev. Lett. **90**, 224501 (2003).
[46]R. B. Bird, C. F. Curtiss, R. C. Armsorong, and O. Hassager, *Dynamics of Polymeric Liquids: Kinetic Theory* (Wiley, New York, 1987).
[47]A. Yethiraj and C. K. Hall, "Monte Carlo simulations of polymers confined between flat plates," Macromolecules **23**, 1865 (1990).
[48]J. T. Stuart, "On the non-linear mechanics of wave disturbances in stable and unstable parallel flows: Part 1. The basic behavior in plane Poiseuille flow," J. Fluid Mech. **9**, 353 (1960).
[49]J. Watson, "On the nonlinear mechanics of wave disturbances in stable and unstable parallel flows: Part 2. The development of a solution for plane Poiseuille and for plane Couette flow," J. Fluid Mech. **9**, 371 (1960).
[50]A. Davey, "On Itoh's finite amplitude stability theory for pipe flow," J. Fluid Mech. **86**, 695 (1978).
[51]V. Kumaran, "Stability of fluid flow through a flexible tube at intermediate Reynolds number," J. Fluid Mech. **357**, 123 (1998).
[52]P. Chokshi and V. Kumaran, "Weakly nonlinear stability analysis of a flow past a neo-Hookean solid at arbitrary Reynolds numbers," Phys. Fluids **20**, 094109 (2008).
[53]C. D. Dimitropoulos, Y. Dubief, E. G. Shaqfeh, and P. Moin, "Direct numerical simulation of polymer-induced drag reduction in turbulent boundary layer flow of inhomogeneous polymer solutions," J. Fluid Mech. **566**, 153 (2006).